Polish Society of Composite Materials
Polskie Towarzystwo Materiałów Kompozytowych

13: 4 (2013) 255-259

COMPOSITES THEORY AND PRACTICE

Dariusz Garbiec[1]*, Mieczysław Jurczyk[2]

[1] *Metal Forming Institute, ul. Jana Pawła II 14, 61-139 Poznan, Poland*
[2] *Poznan University of Technology, Institute of Materials Science and Engineering, ul. Jana Pawła II 24, 60-965 Poznan, Poland*
**Corresponding author. E-mail: dariusz.garbiec@inop.poznan.pl*

Received (Otrzymano) 19.03.2013

Al-SiC COMPOSITES SYNTHESIZED BY THE SPARK PLASMA SINTERING METHOD (SPS)

This work presents the results of studies concerning the production and characterization of Al-SiC composite materials with a 20 and 25% volume fraction of reinforcing phase particles. The spark plasma sintering method (SPS) was applied for the purpose of producing these materials. The final product of the applied process was Al-SiC composites characterized by a density from 2.70 to 2.72 g/cm^3. The results of effective porosity and total porosity measurements are discussed. It was proven that as the content of hard ceramic particles increases in the composite, its apparent density, hardness, and compression strength increase with a simultaneous reduction in tensile strength. For example, the performed tests showed that the composite with the 25% silicon carbide content exhibited the greatest hardness (81.2 HBW 2.5/62.5) and compression strength (315 MPa).

Keywords: spark plasma sintering, composite material, Al-SiC composite

WYTWARZANIE MATERIAŁÓW KOMPOZYTOWYCH Al-SiC METODĄ ISKROWEGO SPIEKANIA PLAZMOWEGO (SPS)

Przedstawiono wyniki badań dotyczących wytworzenia i scharakteryzowania materiałów kompozytowych Al-SiC o 20 i 25% udziale objętościowym cząstek fazy wzmacniającej. Do ich wytworzenia zastosowano metodę iskrowego spiekania plazmowego (SPS). Produktem końcowym zastosowanego procesu były kompozyty Al-SiC charakteryzujące się gęstością wynoszącą od 2,70 do 2,72 g/cm^3. Omówiono wyniki pomiarów porowatości otwartej i całkowitej. Wykazano, iż wraz ze wzrostem zawartości w kompozycie twardych cząstek ceramicznych wzrasta jego gęstość pozorna, twardość oraz wytrzymałość na ściskanie, przy jednoczesnym obniżeniu wytrzymałości na rozciąganie. Przykładowo, przeprowadzone badania wykazały, że największą twardością (81,2 HBW 2,5/62,5) oraz wytrzymałością na ściskanie (315 MPa) charakteryzuje się kompozyt o 25% zawartości węglika krzemu.

Słowa kluczowe: iskrowe spiekanie plazmowe, materiał kompozytowy, kompozyt Al-SiC

INTRODUCTION

The spark plasma sintering method (SPS) is a modern method of rapid pressurized sintering of a wide group of materials, including materials classified as hard-sinterable. In this method, periodically repeated high-current impulses of direct current lasting up to several hundred milliseconds are used to heat compressed powder. As a result of the flow of direct current impulses through graphite tools and the powder consolidated inside of these tools, Joule heat is emitted and realizes the self-heating process of the powder. During the initial sintering period, when the material is still porous, spark discharges take place between compressed powder particles at the instant of the flow of high-current direct current impulses. These discharges remove oxides from the surface of the powder, creating electrical contacts with good conductivity and accelerating diffusion processes. Thanks to this, the activation energy of the diffusion processes is reduced, accelerating the sintering process and limiting grain growth, which is of particular significance in the case when nanometric powders are sintered [1-12].

Metal composite materials are a promising group of engineering materials, among which composites with a light metal matrix, dispersion-reinforced with ceramic particles, enjoy particular interest. Among these materials, the composites used most often in the automotive, aircraft, aerospace, armaments, power, electronic, and precise technologies industries are aluminium-silicon carbide type composites, due to their relatively high strength relative to their low density, resistance to corrosion, and increased wear resistance [13-18].

Barthula et al. [19] sintered Al-SiC composite materials with a 10% weight fraction of silicon carbide using the SPS method. The composite powder was produced by the mechanical synthesis method. The sintering process was performed at a temperature of 500°C, with the application of a pressure equal to 50 MPa. The produced composite materials were characterized by hardness at the level of 280 HV0.1 and Young's modulus equal to 126 GPa. Sintering processes of Al-SiC composite materials by the SPS method with a liquid phase fraction have been presented in works [20, 21]. Sintering temperatures within the range of 1450÷1800°C were applied. It was shown that an increase in pressure decreases the porosity of the sinter. Applied pressure equal to 80 MPa at a sintering temperature of 1650°C made it possible to produce sinters with a porosity of 0.4%. This composite was characterized by a hardness of 222 HV10.

The goal of the studies was to determine the influence of different volume fraction of SiC phase particles on the properties of sintered Al-SiC composite materials produced using the spark plasma sintering method.

TEST METHODOLOGY

Power mixtures with 80 and 75% volume fraction of commercially available aluminum powder (99.7% purity) and 20 and 25% volume fraction, respectively, of silicon carbide powder (98% purity) were prepared. The mixing process was performed conventionally, under dry conditions, in a cylindrical container placed on rollers, at a rotational speed of 30 rpm over a period of 5 h.

The sintering process was performed using an HP D 25 (FCT Systeme GmbH) device. R7710 (SGL Carbon) graphite tools were used for this purpose. The loading chamber in the unit of the graphite tools was filled with a powder mixture of a mass of 43 g. For technological reasons, Papyex N998 (Mersen) graphite foil was placed between the powder mixture and the die and punch. The so-prepared tools were placed in the sintering chamber of the HP D 25 device for the purpose of performing the sintering process, which was realized in a vacuum, at a sintering temperature equal to 600°C under a pressure of 50 MPa. The heating rate was 150°C/min, and the sintering time was 2.5 min. The duration of an impulse was equal to 125 ms, and the interval between impulses was 5 ms. Samples with dimensions of Ø40x12 mm were produced, and samples for the tests were cut out of them using an Electrical Discharge Machining (EDM) device.

Particle grain size distribution analysis was performed using the laser diffraction technique with the application of a Mastersizer 2000 (Malvern) analyzer. X-ray diffraction examinations were conducted using an Empyrean (PANalytical) X-ray diffractometer with CuK_α (λ = 1.54060 Å) radiation in the range of 2Θ angles from 30 to 150°. Microstructure studies were performed on etched specimens (50 ml water, 3 ml hydrochloric acid, 1 ml nitric acid (V), 6 ml of hydrofluoric acid) made from a longitudinal section, over n intervals from 0.5 to 2 minutes, using an Eclipse L150 (Nikon) light microscope. Apparent density and effective porosity measurements were performed using the gravimetric method. The total porosity of the sinters was calculated. An HBW hardness measurement was performed under a load of 613 N over 15 s using a steel ball with a diameter of 2.5 mm. Tensile strength R_m was determined in a static tensile test using an MT5000H (Gatan) micro-tester placed in the chamber of a scanning electron microscope. Hardening curves and compression strength R_c were determined during a static compression test using an Instron 4483 tester.

TEST RESULTS

Particle size distribution

A monomodal band made up of particles with a diameter of 13.2 μm, which make up 10% of the maximum volumetric fraction, can be seen in Figure 1a. 90% of Al powder particles have a diameter of less than 22.2 μm. In turn, the chart in Figure 1b shows that particles with a diameter of 4.4 μm make up 7% of the maximum volumetric fraction. 90% of SiC powder particles have a diameter of less than 17.1 μm.

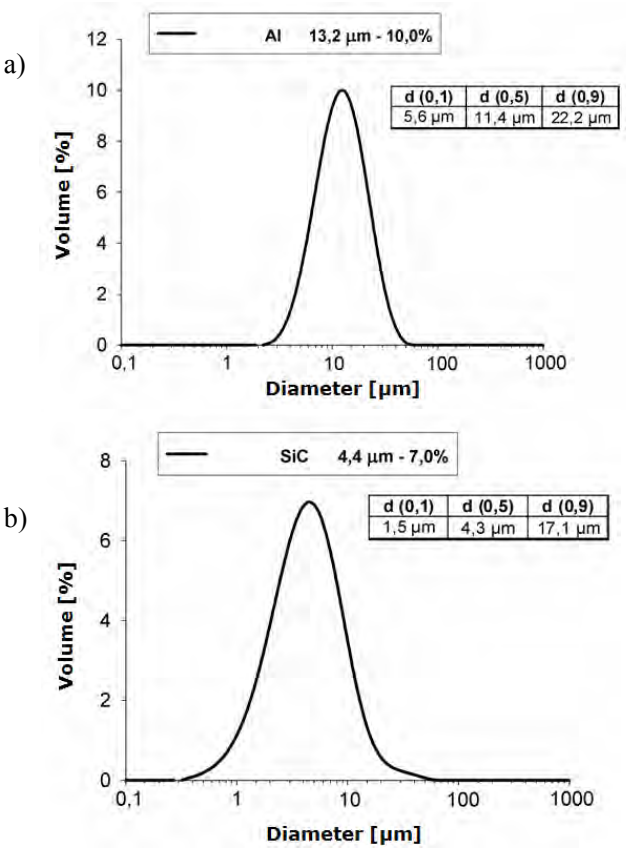

Fig. 1. Particle size distributions relative to volume fractions for: a) Al, b) SiC

Rys. 1. Rozkład wielkości cząstek proszku względem ich udziału objętościowego dla: a) Al, b) SiC

X-ray diffraction examinations

The diffraction patterns of X-ray examinations of the powder mixtures and sinters are presented in Figure 2. The intensity and half-intensity width of Al and SiC peaks before and after SPS consolidation is similar. During the sintering process, no new phases precipitated, similarly to the case of the Al-SiC composites described in [19]. A regular Al phase and a hexagonal 4H-SiC phase are present in the studied composites.

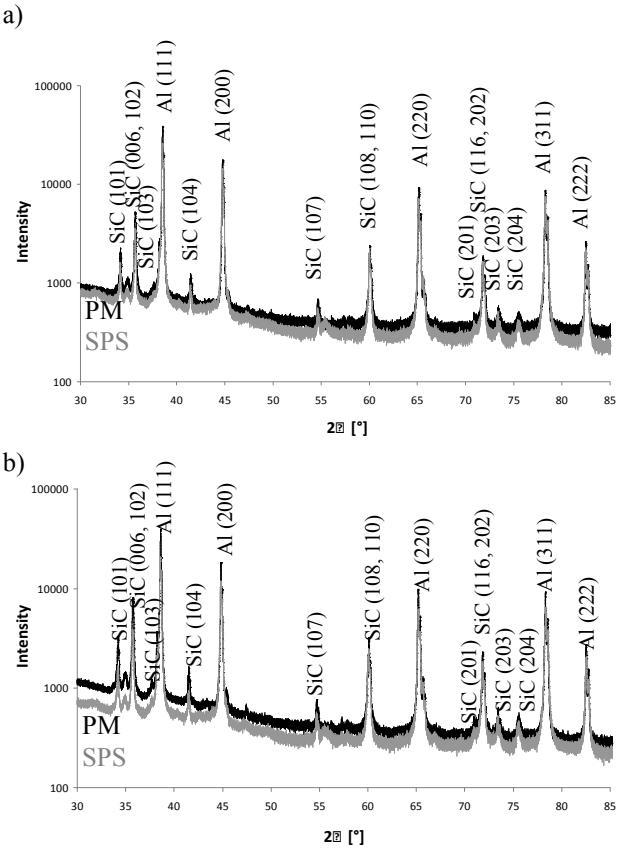

Fig. 2. Diffraction patterns of powder mixture (PM) and sinter (SPS) for: a) Al-SiC 20% and b) Al-SiC 25%

Rys. 2. Dyfraktogramy mieszaniny proszkowej (MP) oraz spieku (SPS) dla: a) Al-SiC 20% i b) Al-SiC 25%

Density and porosity

The results of apparent density and effective and total porosity measurements are presented in Table 1. It can be seen from analysis of the obtained results that an increase in the volumetric share of the ceramic reinforcing phase causes an increase in the apparent density of the composite materials. In the case of the Al-SiC composite with a 20% volume fraction of silicon carbide, density measurements indicate its uniform distribution over the entire volume of the sinter. In turn, the composite with the 25% fraction of reinforcing ceramic phase is characterized by a greater dispersion of density, which may indicate segregation of the SiC particles and the presence of areas with a greater number of pores.

TABLE 1. **Results of apparent density and effective and total porosity measurements of Al-SiC composite materials**

TABELA 1. **Wyniki pomiarów gęstości pozornej i obliczeń porowatości otwartej oraz całkowitej materiałów kompozytowych Al-SiC**

Material	Apparent density [g/cm^3] (σ_{g/cm^3}) ($\sigma_{\%}$)	Effective porosity [%]	Total porosity p [%]
Al-SiC 20%	2.70 (*0.03*) (*1.11%*)	1.76	3.57
Al-SiC 25%	2.72 (*0.17*) (*6.25%*)	1.83	3.94

Al-SiC composite materials produced using the SPS method with the application of high pressure (50 MPa), are characterized by low values of effective porosity (less than 2%). In turn, the total porosity of the sinters is equal to 3.5÷4%, which is indicative of the equal proportion of open to closed pores. In order to compact the material further, the pressure would have to be increased, as is confirmed by the studies presented in [21].

Hardness

Table 2 presents the results of Brinell hardness measurements. The presence of hard ceramic particles affects an increase in the hardness of the composites. As the volume fraction of silicon carbide in the composite increases, the hardness value increases, achieving a value of over 80 HBW 2.5/62.5 in the case of the Al-SiC 25% composite, which constitutes an increase in hardness by more than 2.5 times relative to the hardness of the material of the matrix, which is equal to 31.2 HBW 2.5/62.5.

TABLE 2. **Results of hardness measurements of Al-SiC composite materials**

TABELA 2. **Wyniki pomiarów twardości materiałów kompozytowych Al-SiC**

Material	Hardness [HBW 2.5/62.5] ($\sigma_{HBW\ 2.5/62.5}$) ($\sigma_{\%}$)
Al-SiC 20%	74.8 (*1.15*) (*1.54%*)
Al-SiC 25%	81.2 (*5.29*) (*8.51%*)

Microstructure

Figure 3 presents exemplary microstructures of Al-SiC composites with a 20 (Fig. 3a) and 25% (Fig. 3b) volume share of silicon carbide. On the presented micro-photographs, the light fields represent the Al particles, and the dark fields represent the SiC particles. The small black areas visible on the photograph represent pores. The SiC particles are well wetted by the metal matrix, which is why they are well connected with it. The microstructure observations showed a uniform distribution of reinforcing phase particles in the matrix of the composite. No growth of matrix particles was observed, particularly near their boundaries, in

which the heat-affected zone is the largest during sintering by the SPS method.

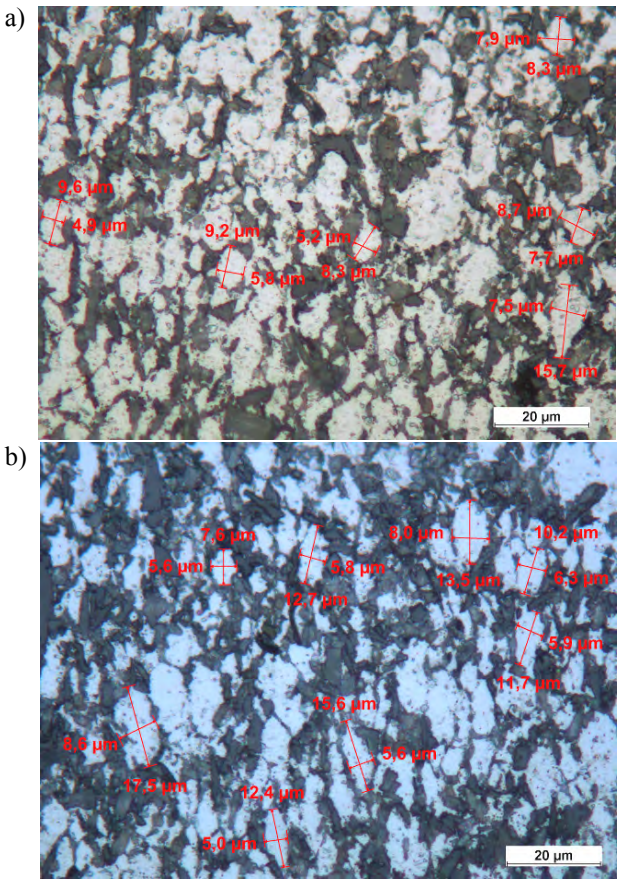

Fig. 3. Composite microstructure: a) Al-SiC 20% and b) Al-SiC 25%

Rys. 3. Mikrostruktura kompozytu: a) Al-SiC 20% i b) Al-SiC 25%

Tensile and compression strength

Based on the obtained results (Table 3), it can be observed that the greatest value of tensile strength R_m (239 MPa) was recorded for composites with the 20% volume fraction of ceramic reinforcing phase particles. An increase in their volume fraction to 25% causes reduction of the R_m value to 218 MPa, which is characterized by a high dispersion of the values. A lower tensile strength may be the result of the material's increased brittleness, with 1/4 of its volume constituted by hard, but not very plastic, silicon carbide particles. During the action of tensile force, these particles are ripped from the material of the matrix, which leads to tearing of the sample at a lower value of tensile force.

In the case of compression strength (Table 3), an increase in the volume fraction of reinforcing phase particles affects an increase in the value of compression strength R_c of the studied composites. The 5% increase in silicon carbide content in the composite by 5%, from 20 to 25%, increases the compression strength by 8%, from 289 to 315 MPa. The greater compression strength is related to the higher content of hard ceramic particles in the composite, however, due to their brittleness, the plastic properties are reduced, which result from the hardening curves of the composite material (Fig. 4).

TABLE 3. **Tensile and compression strength of Al-SiC composite materials**

TABELA 3. **Wytrzymałość na rozciąganie i ściskanie materiałów kompozytowych Al-SiC**

Material	Tensile strength R_m [MPa] (σ_{MPa}) ($\sigma_{\%}$)	Compression strength R_c [MPa] (σ_{MPa}) ($\sigma_{\%}$)
Al-SiC 20%	239 (*2.65*) (*1.11%*)	289 (*2.52*) (*0.87%*)
Al-SiC 25%	218 (*33.98*) (*15.59%*)	315 (*2.88*) (*0.91%*)

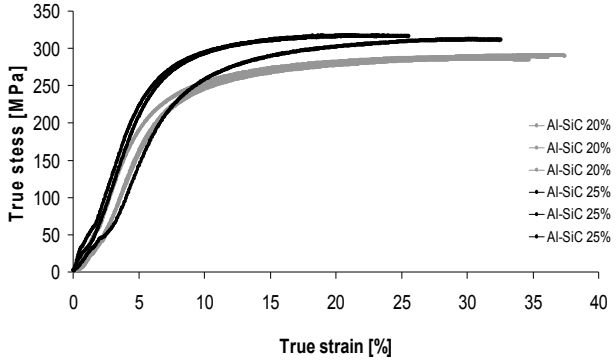

Fig. 4. Hardening curves of compressed Al-SiC composite material with 20 and 25% volume fraction of silicon carbide

Rys. 4. Krzywe umocnienia ściskanego materiału kompozytowego Al-SiC o 20 i 25% udziale objętościowym węglika krzemu

CONCLUSIONS

Al-SiC composite material was produced using the spark plasma sintering method (SPS) at a sintering temperature of 600°C, a pressing force of 50 MPa, a heating rate of 150°C/min, and current parameters of 125:5. As the volume fracture of silicon carbide particles increased in the composite, the hardness and compression strength of the composite also increased. However, the tensile strength was reduced. The composite with the 25% silicon carbide content exhibited the greatest hardness (81.2 HBW) and compression strength (315 MPa). In turn, the greatest tensile strength was achieved by the Al-SiC 20% composite material. Independent of phase compositions, these materials have an equal proportion of the amount of open pores to closed pores. Based on particle size distribution analysis of the powder of the matrix and reinforcing phase, as well as microstructure studies of the sinters, no growth of matrix particles after the SPS sintering method was observed. X-ray examinations did not confirm the formation of new phases.

In further studies, the pressure applied during the spark plasma sintering method should be increased in order to increase the apparent density of the produced composites.

REFERENCES

[1] http://www.sintering.pl

[2] Ûrovskih A.S., Demakov S.L., Kolosova E.V., Osobennosti struktury i fazovogo sostava sloistogo materiala Ti-23Al-26Nb/Al, polčennogo metodom plazmenno-

iskrovogo spekaniâ, Metallovedenie i Termičeskaă Obrabotka 2012, 58, 9, 35-40.

[3] Trombini V., Pallone E.M.J.A., Anselmi-Tamburini U., Munir Z.A., Tomasi R., Characterization of alumina matrix nanocomposite with ZrO_2 inclusions densified by spark plasma sintering, Materials Science and Engineering A 2009, 501, 26-29.

[4] Liu L., Hou Z., Zhang B., Ye F., Zhang Z., Zhou Y., A new heating route of spark plasma sintering and its effect on alumina ceramic densification, Materials Science and Engineering A 2013, 559, 462-466.

[5] Voisin T., Durand L., Karnatak N., Le Gallet S., Thomas M., Le Berre Y., Castagné J.F., Couret A., Temperature control during Spark Plasma Sintering and application to up-scaling and complex shaping, Journal of Materials Processing Technology 2013, 213, 569-278.

[6] Santanach J.G., Estournès C., Weibel A., Chevallier G., Bley V., Laurent C., Peigney A., Influence of pulse current during Spark Plasma Sintering evidenced on reactive alumina-hematite powders, Journal of the European Ceramic Society 2011, 31, 2247-2254.

[7] Santanach J.G., Weibel A., Estournès C., Yang Q., Laurent Ch., Peigney A., Spark Plasma Sintering of alumina: Study of parameters, formal Sintering analysis and hypotheses on mechanism(s) involved in densification and grain growth, Acta Materialia 2011, 59, 1400-1408.

[8] Michalski A., Rosiński M., Metoda impulsowo-plazmowego spiekania: podstawy i zastosowanie, Inżynieria Materiałowa 2010, 31, 7-11.

[9] Rosiński M., Michalski A., Oleszak D., Nanokrystalicznej kompozyty NiAl-TiC spiekane metodą impulsowo--plazmową, Inżynieria Materiałowa 2004, 25, 5, 820-823.

[10] Garbiec D., Rybak T., Heyduk F., Janczak M., Nowoczesne urządzenie do iskrowego spiekania plazmowego proszków SPS HP D 25 w Instytucie Obróbki Plastycznej, Obróbka Plastyczna Metali 2011, t. XXII, 3, 221-225.

[11] Garbiec D., Heyduk F., Spiekanie tytanu i hydroksyapatytu metodą iskrowego spiekania plazmowego, Hutnik - Wiadomości Hutnicze 2012, t. LXXIX, 8, 569-574.

[12] Garbiec D., Heyduk F., Wiśniewski T, Wpływ temperatury spiekania na gęstość, mikrostrukturę i właściwości wytrzymałościowe stopu Ti6Al4V wytwarzanego metodą iskrowego spiekania plazmowego (SPS), Obróbka Plastyczna Metali, 2012, t. XXIII, 4, 265-275.

[13] Bieniaś J., Corrosion studies on aluminium-based metal matrix composites reinforced with graphite, SiC and fly ash particles, Kompozyty (Composites) 2009, 9, 3, 286-290.

[14] Wojciechowski A., Pietrzak K., Sobczak J., Bojar Z., Ocena własności tribologicznych kompozytowych tarcz hamulcowych, Kompozyty (Composites) 2002, 2, 4, 223-228.

[15] Al-Rubaie K.S., Yoshimura H.N., Biasoli de Mello J.D., Two-body abrasive wear of Al-SiC composites, Wear 1999, 233-235, 444-454.

[16] Wojtaszak M., Influence of size of SiC particles on selected properties of aluminium-based composites obtained by extrusion of P/M compacts, Kompozyty (Composites) 2011, 11, 4, 331-335.

[17] Łuczak K., Liberski P., Śleziona J., Wpływ udziału objętościowego i wielkości cząstek na odporność korozyjną kompozytów aluminium-cząstki ceramiczne, Kompozyty (Composites) 2003, 3, 6, 75-78.

[18] Łuczak K., Liberski P., Śleziona J., Ocena odporności korozyjnej kompozytów o osnowie stopu AK12 zbrojonych cząstkami ceramicznymi, Inżynieria Materiałowa 2003, 24, 6, 647-650.

[19] Barthula S., Anandani R.C., Dhar A., Srivastava A.K., Microstructural features and mechanical properties of Al 5083/SiC_p metal matrix nanocomposites produced by high energy ball milling and spark plasma sintering, Materials Science and Engineering A 2012, 545, 97-102.

[20] Zhang Z., Wang F., Luo J., Lee S., Wang L., Microstructures and mechanical properties of spark plasma sintered Al-SiC composites containing high volume fraction of SiC, Materials Science and Engineering A 2010, 527, 7235--7240.

[21] Jaafar M., Bonnefont G., Fantozzi G., Reveron H., Intergranular alumina-SiC micro-nanocomposites sintered by spark plasma sintering, Materials Chemistry and Physics 2010, 124, 377-379.